International Journal of Climatology

RMetS Royal Meteorological Society

Japan's South Foehn on the Toyama Plain: Dynamic or Thermodynamic Theory?

Journal:	*International Journal of Climatology*
Manuscript ID	Draft
Wiley - Manuscript type:	Research Article
Date Submitted by the Author:	n/a
Complete List of Authors:	Hiroyuki, Kusaka; University of Tsukuba, Center for Computational Sciences Nishi, Akifumi; University of Tsukuba, Center for Computational Sciences Kakinuma, Ai; University of Tsukuba, Graduate School of Life and Environmental Sciences Doan, Van; University of Tsukuba, Center for Computational Sciences Onodera, Taira; University of Tsukuba, Graduate School of Life and Environmental Sciences Endo, Shuhei; University of Tsukuba, Graduate School of Life and Environmental Sciences
Keywords:	foehn warming, south foehn, local winds, back trajectory analysis, self-organising map analysis, Weather Research and Forecasting model, Hokuriku
Country Keywords:	Japan

Japan's South Foehn on the Toyama Plain: Dynamic or Thermodynamic?

Hiroyuki Kusaka[1*], Akifumi Nishi[1,†], Ai Kakinuma[2,‡], Quang-Van Doan[1], Taira Onodera[2], and Shuhei Endo[2,‡]

[1] *Center for Computational Sciences, University of Tsukuba, 1-1-1 Tennoudai, Tsukuba, Ibaraki, Japan 305-8577*

[2] *Graduate School of Life and Environmental Sciences, University of Tsukuba, 1-1-1 Tennoudai, Tsukuba, Ibaraki, Japan 305-8577*

[†] *Current affiliation: National Defense Academy of Japan, 1-10-20 Hashirimizu, Yokosuka, Kanagawa, Japan 239-8686*

[‡] *Current affiliation: Japan Weather Association, 3-1-1 Higashi-Ikebukuro, Toshima, Tokyo, Japan Postal Code 170-6055*

***Corresponding author.** H. Kusaka; Tel. +81-29-853-6481; kusaka@ccs.tsukuba.ac.jp;

ORCiD: 0000-0002-0326-7179

Abstract

Japanese society has recently taken a greater interest in foehn warming because it has caused sudden increases in heatstroke among residents and damage to rice crops. This is the first comprehensive climatological study focused on Japan's south foehn, which blows across the Toyama Plain in Hokuriku region. Climatological analyses, including an objective self-organising map (SOM) and subjective analysis of 198 south foehn cases, revealed that ~68.2% of the foehn occurred while an extratropical cyclone was passing in the Sea of Japan. Approximately 19.7% of the remaining foehn blew while an anticyclone covered Japan. Only 5.1% of all foehn events occurred during a typhoon, but very high temperatures occurred when typhoons were approaching. The foehn was observed across all seasons, but it tended to blow more often in spring, when there are many migratory anticyclones and cyclones. Most of the foehn begins at night and ends or pauses during the day. This is due to the removal of the nocturnal stable layer and the development of a local daytime pressure gradient. Surprisingly, thermodynamic-type foehn events accounted for only ~18.7% of all cases, with ~40.0% being typhoon cases. Isentropic drawdown theory provides the primary explanation for Japan's south foehn. Numerical simulations and back trajectory analyses for 55 select foehn cases revealed that the majority of the air particles came from the south and passed straight over the Hida Highlands, between two mountain ranges, as hybrid type of gap and foehn winds.

Keywords: foehn warming, south foehn, local winds, back trajectory analysis, self-organising map analysis, Weather Research and Forecasting model, Hokuriku

Country Keywords: Japan

1. Introduction

Japanese society has recently taken a greater interest in foehn warming. What began this growth was the 2007 revision of Japan's daily maximum temperature record for the first time in 74 years (Takane and Kusaka 2011). In 2018, the record was revised again due to foehn warming (Nishi and Kusaka 2019). Extremely high-temperature, nocturnal events in Niigata Prefecture in 2018 were also caused by foehn warming (Nishi et al. 2019). In Japan, extreme foehn warming causes the incidents of heatstroke to residents, and the high temperatures and dry, strong winds of the foehn cause rice crops to suffer from disease. A recent increase in the number of heatstroke patients and rice-field damage has also increased public interest in the foehn warming.

The term 'foehn' originated from the name of a local wind blowing across the European Alps, but today it is a generic term for any warm, dry, wind descending over the lee side of a mountain. Local winds similar to foehn occur worldwide; a particularly famous example is the Chinook, which blows downwind over the Rocky Mountains (Brinkmann 1974). Studies on the Alps foehn and Chinook have a long history, and several mechanisms have been proposed to explain foehn warming. Among the well-known warming theories, the dynamic warming theory (type I) and thermodynamic warming theory (type II) are the most prominent (Hann 1866; see also Barry 2008; Beran 1967; Richiner and Hächler 2013). The type I theory involves adiabatic compressive warming due to downslope winds. It is also called the 'isentropic drawdown' theory (Elvidge and Renfrew 2016). Type II is the most well-known theory because it is often introduced as a typical example in many introductory textbooks. In this type, precipitation and latent heating over the windward slopes of mountains play an important role in warming. Other theories have also been proposed, including that of Beran (1967), who identified two further mechanisms of warming; in these type III and IV mechanisms, it is important to remove the cold air mass and to prevent nocturnal radiative cooling of the surface layer, respectively.

As the performances of numerical models and computers have improved, two theories of foehn warming during precipitation events over the windward slopes of the mountains have been proposed in recent studies – 'hybrid theory' (Takane et al. 2015) and 'scrambling theory' (Miltenberger et al. 2016). Additionally, Takane and Kusaka (2011) and Elvidge and Renfrew (2016) respectively showed the importance of the sensible heat flux from mountain surfaces and the upper convective layer for foehn warming without precipitation. Other mechanisms were described by Richiner and Hächler (2013).

While there are various mechanisms that may underly foehn warming, the primary one may differ among regions. For example, dynamic mechanisms more frequently underly the Austrian foehn than thermodynamic mechanisms (Seibert 1990; Würsch and Sprenger 2015). In contrast, the Swiss foehn is more clearly characterised by thermodynamic processes, though both types occur (Miltenberger et al. 2016; Würsch and Sprenger 2015).

Past studies on foehn-type winds in various regions have indicated that characteristics such as the most favourable synoptic patterns, flow patterns, and interactions with cold pools, as well as thermally driven mesoscale circulations, differ between the various types of foehns, including the south and north foehns in the Alps (e.g. Cetti et al. 2015; Drobinski et al. 2007; Gohm and Mayr 2004; Haid et al. 2018; Hoinka 1985a, 1985b; Jaubert et al. 2005; Richner and Hächler 2013; Zängl 2003, 2004), Chinook in the Rocky Mountains (Brinkmann 1973, 1974; Durran 1986; Lilly 1978), Santa Ana in California (Hughes and Hall 2010; Raphael 2003; Rolinski et al. 2019), and the New Zealand foehn (McGowan and Sturman 1996, McGowan et al. 2002). Japanese foehns are not as well studied as those in the Alps, the Chinook, or the Santa Ana. However, some headway has been made in previous studies to understand these winds.

Foehn-type winds blow in various places across Japan (Kusaka and Fudeyasu 2017; Yoshino 1975). The northwest foehn that blows across the Kanto Plain in summer blows weakly under the influence of the Pacific High, and foehn warming is caused by a combination of

adiabatic compression heating and surface sensible heating (Nishi and Kusaka 2019; Takane and Kusaka 2011).

The south foehn blows across the Sea of Japan side of Honshu (main island of Japan) (Arakawa et al. 1982; Nishi et al. 2019), Hokkaido (Mori and Sato 2014), and Shikoku (Saito 1994; Saito and Ikawa 1993). The south foehn on the Hokuriku region in Honshu is representative foehns in Japan. Here, the Hokuriku region is located in the Sea of Japan side in the middle part of Honshu (Fig. 1). The south foehn is often observed at the exits of valleys in the plains of Hokuriku region (A, B, and C in Fig. 1b and Fig. 2) and sometimes blows strongly. For example, the speed of the 'Inami-Kaze' (winds in the Inami area) blowing in Tonami Plain is more than 50 m/s (Koyanagi and Kusaka 2019). It is also known that the south foehn in the Hokuriku region blows when an extratropical cyclone passes through the Sea of Japan or when a typhoon approaches Japan (Arakawa et al. 1982; Shibata et al. 2010; Yoshino 1975). As in other areas of the foehn, when wind direction changes rapidly to the south, wind speed increases, and temperature increases simultaneously, and relative humidity changes at almost the same time (Fig. 3). However, it remains unknown whether the foehn blows under other pressure patterns.

South foehn warming may be explained by two types of warming mechanisms – those governed by dynamic theory and thermodynamic theory (Arakawa et al. 1982). However, which is the primary type is unknown, and only a few studies have been conducted on the path of Japan's south foehn (e.g. Arakawa et al. 1982; Ishizaki and Takayabu 2009; Nishi et al. 2019). Arakawa et al. (1982) plotted the distribution of observed surface winds and conjectured that a representative south foehn on the Toyama Plain (B in Fig. 1b) blows due-northward from the Nobi Plain (D in Fig. 1b) to the Toyama Plain through the Hida Highlands. Here, the Hida Highlands is the high altitude areas between the Ryohaku Mountains (F in Fig. 1b) and Hida Mountains (G in Fig. 1b). Ishizaki and Takayabu (2009) simulated two typical south foehns and

supported this proposal. However, only case studies have been employed, while determining the primary path requires more detailed numerical simulations and statistical analyses. As climatological studies on Japan's south foehn are lacking, there are still many unknown aspects of these winds, such as:

(1) Are dynamic or thermodynamic mechanisms more typical of Japan's south foehn?

(2) Is it true that the south foehn only occurs when a cyclone or typhoon approaches?

(3) What is the primary path of the south foehn?

The purpose of this study is to answer these fundamental questions in order to reveal the general characteristics representative of the south foehn on the Toyama Plain in Hokuriku.

The south foehn on the Toyama Plain is called 'Jintsu-Oroshi', in reference to the downslope windstorms blowing in the Jintsu River area. This study is the first complete climatological study of Japan's south foehn. As noted by Richiner and Hächler (2013), insights into natural processes can be gained by statistical analyses of many scenarios, as well as through detailed case studies.

2. Data and Methods

2.1 Study area and dataset

Japan's south foehn is a downslope windstorm from the Backbone Mountain of Japan observed in the coastal areas of the Sea of Japan. It is widely known that one of the areas where the south foehn often blows is the Toyama Plain in the Hokuriku region (e.g. Arakawa et al. 1982; Ishizaki and Takayabu 2009; Shibata et al. 2010). Consequently, this study was focused on the south foehn observed at the Japan Meteorological Agency (JMA) observatory in Toyama Plain. This observatory was selected as the representative observation station in the Hokuriku region, as in previous studies (c.f. Arakawa et al. 1982; Ishizaki and Takayabu 2009; Shibata et al. 2010). Indeed, on days when the south foehn has been recorded at the Toyama observatory, it

126 has usually been observed in other plains across the Hokuriku region (e.g. Arakawa et al. 1982).
127 The target period for this study lasted 10 years, from 2006 to 2015.
128 Surface station, radar, and operational meso-scale analysis data (MANAL), as well as
129 surface weather charts created by the JMA were used in this study to understand the
130 characteristics of Japan's south foehn. The observational sampling intervals were every 10
131 minutes for surface station data, 30 minutes for radar data, 3 hours for objective analytical data,
132 and 12 hours for the weather charts, respectively. The final operational analysis data (FNL)
133 from the National Center for Environmental Prediction (NCEP) collected at a 6-hour interval
134 were also used.
135

136 **2.2 Methodological overview**

137 Prior to our analyses, foehn events occurring between 2006 and 2015 were extracted and the
138 typical synoptic weather patterns causing the foehn were then explored. Seasonal and daily
139 frequencies of the foehn events were surveyed, along with the intensities of foehn warming. In
140 this study, the intensity was defined by the differences between the potential temperatures
141 recorded at the Toyama observatory and those from an observatory on the windward plain. The
142 wind speed during the foehn event was also surveyed. We classified 198 foehn warming events
143 as either thermodynamic and dynamic according to radar and rain gauge data in order to
144 understand the primary mechanism driving foehn warming. Finally, typical paths of the foehn
145 flow were investigated.
146

147 **2.3 Extraction of foehn events**

148 Previously, researchers have proposed extraction methods, definitions, and indices for the
149 Alps foehn (e.g. Drechsel and Mayr 2008; Mayr et al. 2018). While these methods are
150 beneficial, they are not desirable for application to Japan's south foehn because of its local

characteristics. In a previous study on Japan's south foehn, high-temperature and low-humidity days, when winds were blowing from the direction of the mountains, were regarded as foehn occurrence days. (Shibata et al. 2010). However, in this simplified approach, there is a possibility that hot and dry days caused by changes in large-scale phenomena may also be regarded as foehn occurrence days. As Mayr et al. (2018) noted, it is often difficult to objectively differentiate a foehn using the data from only one surface station.

In this study, to reduce the problems afflicting the previous study by Shibata et al. (2010), Japan's south foehn events were defined using data from multiple surface stations, as well as upper-level data. Specifically, an event was defined as a foehn when all of the following four conditions were simultaneously satisfied at the Toyama observatory for two hours or more:

(1) The wind from near-ground level to 900 hPa blew from the mountains (ENE–SSW);

(2) Near-ground and 950-hPa wind speeds exceeded 3 m/s and 5 m/s, respectively;

(3) The potential temperature was 3 K higher than at the observatories on the Nobi Plain, located in the southeast (Pacific Ocean) side of Honshu;

(4) Wind directions changed rapidly, wind speeds increased, and temperatures increased simultaneously, and relative humidity changed at almost the same time.

Conditions (1) and (2) were used to eliminate the cases of land breezes and down-valley winds. These thresholds were determined in consideration of the wind speeds and thicknesses of the thermally induced winds in this area. Condition (3) was used to eliminate warming due to changes in larger scale phenomena, in reference to the methods of Drechsel and Mayr (2008) and Mayr et al. (2018). Condition (4) was used to provide conservative estimates, according to expert opinion. Here, foehn events were detected only from high-temperature days to reduce false positives, although such events on other days may have been missed. High-temperature days were defined as follows:

(1) The temperature deviation, dT (24 hours × 365 days × 15 years of samples), was

calculated from the difference between hourly temperature, T (24 × 365 × 15 samples), and the climate-averaged value of T for each hour and each day, T_C (24 × 365 samples). In short, $dT = T - T_C$ for each hour and day. Here, T_C was smoothed by the Kolmogorov–Zubenko filter (i.e., the simple moving average of 9 days was repeated three times), according to the JMA method (JMA, 2020).

(2) We defined dT_{max} (365 samples) as the daily maximum value of dT.

(3) For each month, the top 20% of days with dT_{max} were extracted as the high-temperature days. As a result, 198 south foehn events were extracted between 2006 and 2015.

2.4 Classification of synoptic weather patterns

Synoptic weather conditions proximal to the timing of foehn onset were investigated to categorise the synoptic patterns. This task was aimed at improving our understanding of the linkages between foehn events and synoptic weather patterns. For our analyses, we employed both subjective, human-made classifications and objective classification via self-organising mapping (SOM). The reasons for using these two approaches were to retain the benefits of each approach, while also reducing the uncertainty of the results. Subjective analyses involved first classifying historical synoptic weather charts, based on visual analyses, into one of five types: (1) extratropical cyclone over the Sea of Japan, (2) anticyclone, (3) typhoon, (4) stationary front, and (5) others. We then counted the frequency of the foehn events appearing in each synoptic weather pattern.

An SOM is a kind of neural network that uses unsupervised learning to produce low-dimensional representations (usually in the form of a two-dimensional map) of high-dimensional input vectors (Kohonen 1982). In climatological studies, the use of SOMs has recently increased and been applied for various purposes, including the recognition of synoptic weather patterns (e.g. Cavazos 2000; Ohba et al. 2016; Ohba and Sugimoto 2020; Rolinski et al.

2019). The SOM analytical procedure this study involved first training the SOM model with the sea level pressure (SLP) data from NCEP (i.e. FNL data proximal to the timing of foehn onset to produce a 3×3 two-dimensional SOM). Here, a total of 496 SLP data points or vectors were used. Each element of the SOM, called a 'node', was initialised with random values and iteratively updated by providing the input SLP vectors. At each iteration, the best-matching unit was selected. The best-matching unit and its neighbouring nodes were then trained to be closer to the input vector. The training process was determined by a learning rate and a 'neighbourhood function'. The initial learning rate was 0.1, and it then decreased exponentially, while the neighbourhood function was Gaussian; this configuration is standard in SOM analyses. We then classified the 198 foehn events into 9 SOM node patterns before finally counting the frequency of the foehn events corresponding to each SLP pattern obtained from the SOM analysis.

2.5 Back trajectory analysis and numerical simulations

Back trajectory analysis was performed to understand the typical paths of foehn flow. Prior to trajectory analysis, numerical simulations were conducted with the Weather Research and Forecasting (WRF) model and predictable variables were output every three minutes. Subsequently, the 55 foehn cases that were highly reproducible were selected for back trajectory analysis. Particles of 72 foehns were released from 100 m and 500 m above sea level around the Toyama observatory.

The simulation domain of the WRF model is shown in Fig. 1b. The horizontal grid spacing was 3 km and the number of vertical layers was 70. Dudhia's simple scheme was used to calculate the shortwave radiation (Dudhia 1989), the Rapid Radiative Transfer Model (RRTM) was used to calculate the longwave radiation (Mlawer et al. 1997), and the WRF single-moment six-class cloud microphysics scheme (WSM6) was used to model the physical processes of

clouds (Hong et al. 2004). Additionally, the Yonsei University (YSU) scheme was employed to account for boundary layer turbulence (Hong et al. 2006), and the Noah-Multiparameterisation (Noah-MP) land surface model was used for ground surface processes (Chen and Dudhia 2001). The topographical and land use data used in the simulation were created from the National Land Numerical Information data of Japan (Ministry of Land, Infrastructure, Transport and Tourism, 2020). The initial and boundary conditions were created from the NCEP-FNL data.

3. Results and Discussion

3.1 Characteristic synoptic weather patterns

Does Japan's south foehn really only blow while cyclones or typhoons are approaching? We sought to answer this question by reviewing weather charts from the onsets of 198 past foehn events between 2007 and 2015. Figure 4 illustrates four types of typical weather charts. Here, the extratropical cyclone-type pattern was defined as the chart type when a cyclone was passing through the Sea of Japan and the Hokuriku region was under the influence of the cyclone. In the typical case, the Hokuriku region was covered by warm-sector air (Fig. 4a). The tropical typhoon-type was defined as the chart type when a typhoon was approaching Japan and the Hokuriku region was affected by the advection of warm and moist air from the south (Fig. 4b). The anticyclone-type was defined as the chart type when an anticyclone was centred on the Pacific Ocean side of the Honshu and the Hokuriku region was under the influence of the anticyclone (Fig. 4c). The stationary front-type was defined the chart type in which a stationary front existed near Japan (Fig. 4d).

Table 1 summarises the frequency with which each weather chart pattern (synoptic pattern) appeared near the time of foehn onset between 2007 and 2016. This table also contains information about the type of foehns. Of the weather charts proximal to foehn onset, the most frequent synoptic pattern was that of an extratropical cyclone. The total number of this type

pattern was 135 and accounted for 68.2% of all foehn events. This result agrees well with the expectations of many weather forecasters and researchers (e.g., Nitta and Tatehira 2000; Yoshino 1975). The second most common synoptic pattern was the anticyclone-type. The total number of this type was 39 and accounted for 19.7% of all foehn events. This finding resulted from carefully analysing weather maps for many foehn cases in this study. The third most common pattern was the typhoon-type, for which there were ten events, accounting for 5.1% of the total. It is noteworthy that hazardous foehns, which satisfy the 95th percentile of the daily maximum temperature, were all associated with typhoon-type weather patterns.

Until this study, it was thought that Japan's south foehn only occurred under the influence of extratropical cyclones or typhoons. However, the result of our analyses reveal that the south foehn blows even under the control of anticyclones, with a relative frequency of ~1/3 that of the extratropical cyclone-type and nearly four times that of the typhoon-type. Some researchers have suggested that the extratropical cyclone and anticyclone types are the same, and thus there is no reason to distinguish them. In answer to the veracity of this claim, this study confirmed the existence of a discrete anticyclone-type pattern via SOM techniques.

Figure 5 illustrates the nine synoptic weather patterns generated via SOM analysis. In the SOMs, close patterns are allocated into close nodes, and vice versa. Nodes 2 and 7 show typical extratropical cyclone-type patterns, as do Node 5 and Node 8. Indeed, all of the patterns are allocated close to Nodes 2 and 7 in the SOM. In contrast, in Node 0, the entire Hokuriku region and Backbone Mountain appear to lie under the high-pressure system extending over the West Pacific. Thus, this node, which is distinct from Nodes 2 and 7 of the extratropical cyclone-type, can be recognised as anticyclonic. It can also be seen that Node 0 is allocated far away from Nodes 2 and 7 in the SOM. The results from the objective pattern analysis via SOM supported those achieved via subjective analysis, in which there were also anticyclonic synoptic weather patterns observed in the blowing of this wind.

276

277 **3.2 Seasonal and hourly frequencies and intensities of foehns**

278 Figure 6a shows the distribution of the monthly frequency for the 198 south foehn events
279 between 2006 and 2015. Seasonally, the south foehn most frequently occurred in spring. The
280 frequencies of occurrence in March, April, and May accounted for 11.9%,13.2%, and 11.7% of
281 all occurrences, respectively. As is well-known, extratropical cyclones and anticyclones
282 frequently pass over Japan in Spring. Extratropical cyclones often produce strong north–south
283 pressure gradients across Japan's Backbone Mountain and southerly winds in the warm sector
284 (Fig. 4a). Anticyclones in the Pacific Ocean also produce north–south pressure gradients. The
285 other noteworthy seasonal feature of the south foehn is its relatively low frequency in June. One
286 reason for this is that the Baiu Front stays over Japan in June.

287 Figure 6b shows the duration of the south foehn. Most south foehns continue to blow for 5–
288 24 hours. The onset of Japan's south foehns mainly occurs when the Hokuriku region is in the
289 warm sector of an extratropical cyclone and the direction of the wind approaching from the
290 Backbone Mountain range changes to the south. Then, the foehn event ends just after the cold
291 front passes over the Hokuriku region. Thus, its resulting duration is reasonable. However, it is
292 also noteworthy that foehn warming is sometimes stopped due to local effects, such as sea
293 breezes.

294 Figure 6c shows the clear diurnal variation in foehn activity. The results show that the south
295 foehn occurs more often during the night-time and less often in the day. This tendency is
296 particularly found in anticyclone-type foehns (Table 2). One reason for this is that strong winds
297 remove the cold air layer at night when the foehn begins, while another cause may be the
298 influence of thermally driven local circulation. The Toyama Plain faces Toyama Bay on its
299 north side and is adjacent to the Hida Highlands on its south side (Fig. 1b). Therefore, sea
300 breezes and up-valley winds can blow during the day and land breezes and down-valley winds

301 can blow at night. Minimally, a local pressure gradient can be generated in a given direction to
302 blow these winds, and such winds or local pressure gradients may break or terminate foehn
303 winds. The hourly frequencies of the onset and cessation of foehns support this notion (Fig. 7).
304 The modal onsets and end times of south foehns are 22:00 Japan Standard Time (JST) and
305 11:00 JST, respectively.

306 Another important aspect of foehn behaviour is the intensity. In this study, we used the
307 potential temperature difference between the Toyama observatory and windward surface stations
308 ($\Delta\theta$) in order to assess the thermal behaviour (Fig. 8a). The mean of potential temperature
309 difference between the station on the Toyama Plain and Nobi Plain, $\Delta\theta$ was 5.6K. This tendency
310 did not depend on the synoptic weather pattern (Table 2); however, 57% (4 of 7 cases) of the
311 south foehns, which bring high temperatures (i.e. such that increase the risk of heatstroke in
312 humans) over 35℃ to Toyama City, were typhoon-type foehns. Considering that such foehns
313 accounted for only 5.1% of all foehn activity, it can be said that typhoon-type foehns are more
314 likely to bring dangerously high temperatures than other types. These high temperatures are likely
315 to be influenced not only by the foehn, but also by the advection of warm air from the typhoon.

316 When examining foehn intensity, the wind speed must also be considered (Fig. 8b). The mean
317 wind speed in this study was 6.3 m/s. For the very high-wind-speed cases (90th percentile), wind
318 speeds were >9.3 m/s. This tendency also did not depend on the synoptic weather pattern. The
319 reason why the wind speeds of typhoon-type foehns were not as high is those in the centres of the
320 typhoons was because the typhoons were located far from the Hokuriku region when the foehns
321 occurred.

322

323 **3.3 Contribution of thermodynamically controlled foehns**

324 Which is the primary type of the south foehn, dynamic or thermodynamic? To answer this
325 question, all 198 foehn cases were first classified into those with precipitation on the windward

slope of the mountains and those without. Surprisingly, most of the foehns (81.3%) were dynamical and occurred without precipitation (Table 1). This type accounted for 79.3% of all of the foehns associated with extratropical cyclones, and 60.0% for those associated with typhoons. All of the foehns (i.e. 100%) associated with anticyclones were recognised as dynamical in nature. These results indicate that the more famous thermodynamic theory, at least in the case of the southern foehn in Japan, does not govern primarily, but rather dynamic theory predominates.

As Takane et al. (2015) and Miltenberger et al. (2016) noted, not all air particles are unaffected by thermodynamic processes, even if they pass through windward precipitation areas. Therefore, in some of the precipitation cases, it cannot be conclusively determined that the primary warming process was thermodynamic rather than purely dynamical in nature. In this study, foehns without precipitation were recognized as the dynamical type, but they possibly include removal of cold air near the ground surface, for instance, nocturnal surface inversion layer.

Focusing extratropical cyclonic foehns, we analysed the relationship between cyclone location and foehn-type. The location of the cyclone centre differed between dynamical and thermodynamic foehns (Fig. 9), and there was a tendency for precipitation to occur near cyclones, with no precipitation far from them. This is reasonable from the viewpoint of a synoptic field. Generally, no precipitation is likely to occur when Hokuriku sits within a warm-sector region of a cyclone, while precipitation is likely to occur when the centre of a cyclone is passing near Hokuriku. To obtain more robust conclusions, more data on thermodynamical foehns are needed.

3.4 Results of back trajectory analysis

The results of back trajectory analyses revealed that the south foehns mainly took three

paths. Most of the anticyclonic foehns with dynamic warming processes (90% for all cases) involved air particles coming from the south and passing straight over the gap between the Hida Highlands and Hida Mountains, and then descending from ~1500 m (Fig. 10). Air particles did not flow from the bottom of the Hida Highlands; thus, the airflows were not cold-drainage-currents but hybrid of foehn winds and gap winds.

Most of the cyclone-type foehns with dynamic warming process (77% for all cases) exhibited similar paths as the anticyclone-type foehns (Fig. 11a). However, there were two other paths that were observed. One involved air particles coming from the west hitting the Hida Mountains, turning northward, and then descended from ~1500 m (10% for all cases) (Fig. 11b). A part of the dynamical effects was the barrier jet. The other pattern observed involved air particles coming from the east hitting the Ryohaku Mountains, turning northward, and then descending from 1500 m (11% for all cases) (Fig. 11c). These latter paths were newly recognised in this study. In the cyclonic foehns with precipitation over the windward areas, the courses were similar to those of the cyclonic foehns without precipitation, but air particles experienced uplift on the windward slopes (Fig. 12).

3.5 Comparison with the results of previous studies

We compared the results from this study to those from two previous studies. Shibata et al. (2010) and Arakawa et al. (1982) stated that Japan's south foehn blows in response to extratropical cyclones and typhoons; however, we found that ~20% of all foehn events in a 10-year period occurred under the influence of anticyclones. In the commentaries of weather forecasters and textbook descriptions, foehn warming in Japan has mostly been explained according to thermodynamic theory, but this study revealed that thermodynamic theory could explain only 20% of the 198 documented foehn warming events between 2006 and 2015. In particular, this theory could not explain foehn warming under the control of anticyclones. This

is much less than the chances of being explained by thermodynamic theory than for foehn warming in the European Alps found by Seibert (1990) and Würsch and Sprenger (2015).

Arakawa et al. (1982) supposed, from surface meteorological station data, that the foehns blowing on the Toyama Plain are derived from winds on the Nobi Plain, which cross the Hida Highlands and reach Toyama. Ishizaki and Takayabu (2009) simulated this course, and the results of this study strongly support their findings and enhance their robustness by the addition of statistical analyses. We also found that there were two other minor paths for cyclonic foehns. In contrast, the path to reach the Toyama Plain by detouring to the west of the Ibuki and Ryohaku mountains (E and F in Fig. 1b), as estimated in a previous study by Ishizaki and Takayabu (2009), was not supported in this study. However, in the study by Ishizaki and Takayabu (2009), there was a problem in that they began back trajectory analysis after foehns terminated and changed to westerly winds. Indeed, Ishizaki and Takayabu (2009) could not recognise such foehns at all. It is thus reasonable that this course did not appear in this study.

4. Conclusions

The characteristics of Japan's south foehns that blow in the Hokuriku region were revealed in this study, which is the first comprehensive climatological study on foehn warming events in this region. Prior to our analyses, 198 foehn events were extracted from the top 20% high-temperature days from 2006–2015. We found that most of Japan’s south foehns tend to occur under three synoptic weather conditions: extratropical cyclones in the Sea of Japan (68.2% of all foehn events), anticyclones south of Japan (19.7%), and typhoons around Japan (5.1%).

The potential temperature in the foehn area was, on average, 5.6℃ higher than on the windward plain. The mean wind speed was 6.3 m/s, and most of the hazardous foehns, whose daily maximum temperatures exceeded 35℃, were caused by typhoons. Japan’s south foehns are mostly onset at night and end or pause during the day. A possible reason for this behaviour

401 is the removal of the nocturnal stable layer and development of daytime local pressure
402 gradients. South foehns occurred in all of the years sampled and the main foehn season was
403 spring.

404 The primary theory underlying foehn warming is the isentropic drawdown that combats
405 adiabatic compression of the air due to decent. Surprisingly, thermodynamic theory could
406 explain only 18.7% of the foehn warming events and only 40.0% of those induced by typhoons.
407 Back trajectory analyses showed that most of the air particles descend from the Hida Highlands
408 between the two mountain ranges, like as hybrid type of foehn winds and gap winds. It is
409 noteworthy that the air particles did not flow within the valley, but rather above it. Combined,
410 these findings provide a holistic view of the mechanisms underlying foehn warming on the
411 Toyama Plain, which may be used to predict the occurrence of dangerously high temperatures
412 and thus, to mitigate the impacts of such extremes on residents and rice crops.
413

414 **Acknowledgements**

415 This work was supported by Cabinet Office, Government of Japan, Cross-ministerial Strategic
416 Innovation Promotion Program (SIP), “Technologies for creating next-generation agriculture,
417 forestry and fisheries” (funding agency: Bio-oriented Technology Research Advancement
418 Institution, NARO). Part of this work is based on results obtained from a project commissioned
419 by the New Energy and Industrial Technology Development Organization (NEDO). Part of this
420 research was performed by the Environment Research and Technology Development Fund
421 JPMEERF20192005 of the Environmental Restoration and Conservation Agency of Japan. We
422 thank Yuma Imai, Shingo Nakamura, Tomoka Maeda, and Miru Maebata for their help in
423 producing the figures, as well as Hiroki Kobayashi and Ryuhei Kimura for their assistance in
424 confirming our observations.
425

426

427 **Figure Captions**

428 **Figure 1.** (a) Topography around the main island of Japan (i.e. Honshu). (b) Central region of
429 Honshu. The area near the coast of the Sea of Japan in Fig. 1b corresponds to the Hokuriku
430 region. The red circles, A, B, C, and D, represent the Fukui Plain, Toyama Plain, Itoigawa
431 Area, and the Nobi Plain, respectively. The black circles, E, F, and G represent the Ibuki
432 Mountains, Ryohaku Mountains, and Hida Mountains, respectively. The highlands between
433 F and G are called the 'Hida Highlands'.

434 **Figure 2.** Example distributions of near-surface (a) temperatures and (b) winds obtained from
435 observations during cyclone-induced south foehn events. The solid lines indicate the
436 topography (contour intervals of 200 m).

437 **Figure 3.** Time series of (a) temperature and relative humidity and (b) wind speed and direction
438 near the surface at the Toyama observatory for cyclone-induced foehns. Thick and thin lines
439 in (a) indicate temperature and relative humidity, respectively. Solid line and vector in (b)
440 indicate wind speed and wind direction, respectively.

441 **Figure 4.** Example synoptic weather charts during foehn events: (a) extratropical cyclone; (b)
442 typhoon; (c) anticyclone; (d) stationary front.

443 **Figure 5.** Self-Organised Maps of Nodes 0–8. Maps indicate the sea level pressure patterns
444 proximal to the timing of foehn onset (contour intervals of 4 hPa).

445 **Figure 6.** Relative frequencies and durations of Japan's south foehns on the Toyama Plain: (a)
446 monthly; (b) duration; (c) hourly. Grey bars of (a) indicate the data collected at the foehn
447 onsets. Grey bars of (b) and (c) indicate the data collected during foehn events.

448 **Figure 7.** Relative frequencies of the onset (black bars) and end (grey bars) times of Japan's
449 south foehns on the Toyama Plain.

450 **Figure 8.** Relative frequencies of the intensity of Japan's south foehns. (a) Potential temperature

difference between the stations on the Toyama Plain and Nobi Plain. (b) Wind speed at the Toyama observatory. Grey bars indicate the data collected during foehn events.

Figure 9. Location of the cyclone centres proximal to foehn onset for cyclone-type foehns (a) without precipitation and (b) with precipitation. Color scales indicate the number of cyclones at each location.

Figure 10. Examples of anticyclonic foehn trajectories without precipitation on the windward side. Colored lines indicate the altitude of the trajectories. Grey scales indicate the topography (contour intervals of 250 m).

Figure 11. Examples of cyclonic foehn trajectories without precipitation on the windward side: (a) south course; (b) west course; (c) east course. Colored lines indicate the altitude of the trajectories. Grey scales indicate the topography (contour intervals of 250 m).

Figure 12. Examples of cyclonic foehn trajectories with precipitation on the windward side: (a) south course; (b) west course; (c) east course. Colored lines indicate the altitude of the trajectories. Grey scales indicate the topography (contour intervals of 250 m).

References

Arakawa, S., Yamada, K. and Toya, T. (1982) A study of foehn in the Hokuriku district using the AMeDAS data. *Papers in Meteorology and Geophysics*, 33, 149-163. https://doi.org/10.2467/mripapers.33.149.

Barry, G. R. (2008) *Mountain Weather and Climate*, 3rd Edition. Cambridge: Cambridge University Press. 506 pp. https://doi.org/10.1017/CBO9780511754753.

Beran, D. W. (1967) Large amplitude lee waves and chinook winds. *Journal of Applied Meteorology*, 6, 865-877. https://doi.org/10.1175/1520-0450(1967)006<0865:LALWAC>2.0.CO;2.

476 Brinkmann, W. A. R. (1973) A climatological study of strong downslope winds in the Boulder
477 area. *NCAR Cooperative Thesis* No.27/INSTARR Occasional Paper No.7, University of
478 Colorado, 229 pp.
479 Brinkmann, W. A. R. (1974) Strong downslope winds at Boulder, Colorado. *Monthly Weather*
480 *Review*, 102, 592-602.
481 https://doi.org/10.1175/1520-0493(1974)102<0592:SDWABC>2.0.CO;2.
482 Cavazos, T. (2000) Large-scale circulation anomalies conducive to extreme precipitation events
483 and derivation of daily rainfall in northeastern Mexico and southeastern Texas. *Journal of*
484 *Climate*, 12, 1506–1523.
485 https://doi.org/10.1175/1520-0442(1999)012<1506:LSCACT>2.0.CO;2.
486 Cetti, C., Buzzi, M. and Sprenger, M. (2015) Climatology of Alpine north foehn. *Scientific*
487 *Report MeteoSwiss*, 100, 76pp.
488 Chen, F. and Dudhia, J. (2001) Coupling an advanced land-surface/hydrology model with the
489 Penn State/NCAR MM5 modeling system. Part I: Model description and implementation.
490 *Monthly Weather Review*, 129, 569–585.
491 https://doi.org/10.1175/1520-0493(2001)129<0569:CAALSH>2.0.CO;2.
492 Drobinski, P., R. and co-authors (2007) Foehn in the Rhine valley during MAP: A review of its
493 multiscale dynamics in complex valley geometry. *Quarterly Journal of the Royal*
494 *Meteorological Society*, 133, 897-916. https://doi.org/10.1002/qj.70.
495 Drechsel, S. and Mayr, G. (2008) Objective forecasting of foehn winds for a subgrid-scale
496 alpine valley. *Weather and Forecasting*, 23 (2), 205–218.
497 https://doi.org/10.1175/2007WAF2006021.1.
498 Dudhia, J. (1989) Numerical study of convection observed during the Winter Monsoon
499 Experiment using a mesoscale two–dimensional model. *Journal of the Atmospheric*
500 *Sciences*, 46, 3077–3107.

https://doi.org/10.1175/1520-0469(1989)046<3077:NSOCOD>2.0.CO;2.

Durran, D. R. (1986) Another look at downslope windstorms. Part I: The development of analogs to supercritical flow in an infinitely deep, continuously stratified fluid. *Journal of the Atmospheric Sciences*, 43, 2527-2543. DOI: 10.1175/1520-0469(1986)043<2527:ALADWP>2.0.CO;2.

Elvidge, A. D. and Renfrew, I. A. (2016) The causes of foehn warming in the lee of mountains. *Bulletin of the American Meteorological Society*, 97, 455–466. https://doi.org/10.1175/BAMS-D-1400194.1.

Gohm, A. and Mayr, G. J. (2004) Hydraulic aspects of föhn winds in an alpine valley. *Quarterly Journal of the Royal Meteorological Society*, 130, 449–480. https://doi.org/10.1256/qj.03.28.

Hann, J. (1866) Zur Frage u¨ber den Ursprung des Fo¨hns. *Zeitschrift der Österreichischen Gesellschaft für Meteorologie*, 1, 257–263.

Haid, M., Gohm A., Umek L., Ward H. C., Muschinski T., Lehner L., and Rotach M. W. (2018) Foehn-cold pool interactions in the Inn Valley during PIANO IOP2. *Quarterly Journal of the Royal Meteorological Society*, 146, 1232-1263. https://doi.org/10.1002/qj.3735.

Hoinka, K. P. (1985a) What is a foehn clearance? *Bulletin of the American Meteorological Society*, 66, 1123-1132. https://doi.org/10.1175/1520-0477(1985)066<1123:WIAFC>2.0.CO;2.

Hoinka, K. P. (1985b) Observation of the airflow over the alps during a foehn event. *Quarterly Journal of the Royal Meteorological Society*, 111, 199-224. https://doi.org/10.1002/qj.49711146709.

Hong, S. Y., Dudhia, J. and Chen, S. H. (2004) A revised approach to ice microphysical processes for the bulk parameterization of clouds and precipitation. *Monthly Weather Review*, 132, 103–120.

https://doi.org/10.1175/1520-0493(2004)132<0103:ARATIM>2.0.CO;2.

Hong, S. Y., Noh, Y. and Dudhia, J. (2006) A new vertical diffusion package with an explicit treatment of entrainment processes. *Monthly Weather Review*, 134, 2318–2341. https://doi.org/10.1175/MWR3199.1.

Hughes, M. and Hall, A. (2010) Local and synoptic mechanisms causing Southern California's Santa Ana winds. *Climate Dynamics*, 34, 847–857. https://doi.org/10.1007/s00382-009-0650-4.

Ishizaki, N. and Takayabu, I. (2009) On the warming events over Toyama Plain by using NHRCM. *SOLA*, 5, 129-132. https://doi.org/10.2151/sola.2009–033.

Japan Meteorological Agency (2020) Explanation of meteorological observation statistics. https://www.data.jma.go.jp/obd/stats/data/kaisetu/shishin/shishin_all.pdf (in Japanese).

Jaubert, G., Bougeault, P., Berger, H., Chimani, B., Flamant, C., Häberli, C., Lothon, M., Nuret, M. and Vogt, S. (2005) Numerical simulation of meso-gamma scale features of föhn at ground level in the Rhine valley. *Quarterly Journal of the Royal Meteorological Society*, 131, 1339-1361. https://doi.org/10.1256/qj.03.197.

Kohonen, T. (1982) Self-organized formation of topologically correct feature maps. *Biological Cybernetics*, 43, 59-69. https://doi.org/10.1007/BF00337288.

Koyanagi, T. and Kusaka, H. (2019) A climatological study of the strongest local winds of Japan "Inami-kaze". *International Journal of Climatology*, 40(2), 1007-1021. https://doi.org/10.1002/joc.6252.

Kusaka, H. and Fudeyasu, H. (2017) Review of downslope windstorms in Japan. *Wind and Structures*, 24(6), 637-656. https://doi.org/10.12989/was.2017.24.6.637.

Lilly, D. K. (1978) A severe downslope windstorm and aircraft turbulence event induced by a mountain wave. *Journal of the Atmospheric Sciences*, 35, 59-77. https://doi.org/10.1175/1520-0469(1978)035<0059:ASDWAA>2.0.CO;2.

551 Mayr, G. J., Plavcan, D., Armi, L., Elvidge, A., Grisogono, B., Horvath, K., Jackson, P.,
552 Neururer, A., Seibert, P., Steenburgh, J. W., Stiperski, I., Sturman, A., Vecenaj, Z.,
553 Vergeiner, J., Vosper, S. and Zängl, G. (2018) The community foehn classification
554 experiment. *Bulletin of the American Meteorological Society*. 99, 2229-2235.
555 https://doi.org/10.1175/BAMS-D-17-0200.1.
556 McGowan, H. A. and Sturman, A. P. (1996) Regional and local scale characteristics of foehn
557 wind events over the South Island of New Zealand. *Meteorology and Atmospheric Physics*,
558 58, 151-164. https://doi.org/10.1007/BF01027562.
559 McGowan, H. A., Sturman, A. P., Kossmann, M. and Zawar-Reza, P. (2002) Observations of
560 foehn onset in the Southern Alps, New Zealand. *Meteorology and Atmospheric Physics*, 79,
561 215-230. https://doi.org/10.1007/s007030200004.
562 Miltenberger, A. K., Reynolds, S. and Sprenger, M. (2016) Revisiting the latent heating
563 contribution to foehn warming: Lagrangian analysis of two foehn events over the Swiss
564 Alps. *Quarterly Journal of the Royal Meteorological Society*, 142, 2194-2204.
565 https://doi.org/10.1002/qj.2816.
566 Mlawer, E. J., Taubman, S. J. Brown, P. D. Iacono, M. J. and Clough, S. A. (1997) Radiative
567 transfer for inhomogeneous atmospheres: RRTM, a validated correlated–k model for the
568 longwave. *Journal of Geophysical Research*, 102, 16663–16682.
569 https://doi.org/10.1029/97JD00237.
570 Mori, K. and Sato, T. (2014) Spatio-temporal variation of high-temperature events in Hokkaido,
571 North Japan. *Journal of the Meteorological Society of Japan*, 92, 327-346.
572 https://doi.org/10.2151/jmsj.2014-404.
573 Nishi, A. and Kusaka, H. (2019) Effect of foehn wind on record-breaking high temperature
574 event (41.1 degrees C) at Kumagaya on 23 July 2018. *SOLA*, 15, 17-21.
575 https://doi.org/10.2151/sola.2019-004.

576 Nishi, A., Kusaka, H., Vitanova, L. L., Imai, Y. (2019) Contributions of foehn and urban heat
577 island to the extreme high-temperature event in Niigata city during the night of 23–24
578 August 2018. *SOLA*, 15,132-136. https://doi.org/10.2151/sola.2019-024.
579 Nitta, T. and Tatehira, R. (2000) *Techniques of the weather forecasting: for the weather*
580 *forecasters.* Tokyo: Tokyo-do Press. 343pp. (in Japanese).
581 Ohba, M., Nohara, D. and Kadokura, S. (2016) Impacts of Synoptic Circulation Patterns on
582 Wind Power Ramp Events in East Japan. *Renewable Energy*, 96, 591–602.
583 https://doi.org/10.1016/j.renene.2016.05.032.
584 Ohba, M. and Sugimoto, S. (2020) Impacts of climate change on heavy wet snowfall in Japan.
585 *Climate Dynamics*, 54, 3151–3164. https://doi.org/10.1007/s00382-020-05163-z.
586 Raphael, M. N. (2003) The Santa Ana winds of California. *Earth Interactions*, 7(8), 1-13.
587 https://doi.org/10.1175/1087-3562(2003)007<0001:TSAWOC>2.0.CO;2.
588 Richiner, H. and Hächler, P. (2013) Understanding and forecasting Alpine foehn. *Mountain*
589 *Weather Research and Forecasting* (Chow, F. K., De Wekker, S. F. J., and Snyder, B. J.
590 Editors). Dordrecht: Springer, 219-260. https://doi.org/10.1007/978-94-007-4098-3_4.
591 Rolinski, T., Capps, S. B. and Zhuang, W. (2019) Santa Ana winds: A descriptive climatology.
592 *Weather and Forecasting*, 34(2), 257–275. https://doi.org/10.1175/WAF-D-18-0160.1.
593 Saito, K. and Ikawa, M. (1993) A numerical study of the local downslope wind "Yamaji-kaze"
594 in Japan. Part 2: Non-linear aspect of the 3-D flow over a mountain range with a col.
595 *Journal of the Meteorological Society of Japan*, 69(1), 31-56.
596 https://doi.org/10.2151/jmsj1965.69.1_31.
597 Saito, K. (1994) A numerical study of the local downslope wind “Yamaji-kaze” in Japan Part 3:
598 Numerical Simulation of the 27 September 1991 Windstorm with a Non-hydrostatic Multi-
599 nested Model. *Journal of the Meteorological Society of Japan*, 72(2), 301-329.
600 https://doi.org/10.2151/jmsj1965.72.2_301.

601 Seibert, P. (1990) South foehn studies since the ALPEX experiment. *Meteorology and*
602 *Atmospheric Physics*, 43, 91-103. https://doi.org/10.1007/BF01028112.
603 Shibata, Y., Kawamura, R. and Hatsushika, H. (2010) Role of large-scale circulation in
604 triggering foehns in the hokuriku district of japan during midsummer. *Journal of the*
605 *Meteorological Society of Japan*, 88(3), 313-324. https://doi.org/10.2151/jmsj.2010-304.
606 Takane, Y. and Kusaka, H. (2011) Formation mechanisms of the extreme high surface air
607 temperature of 40.9°C, observed in the Tokyo metropolitan area: Considerations of dynamic
608 foehn and foehnlike wind. *Journal of Applied Meteorology and Climatology*, 50(9), 1827-
609 1841. https://doi.org/10.1175/JAMC-D-10-05032.1.
610 Takane, Y., Kusaka, H. and Kondo, H. (2015) Investigation of a recent extreme
611 high-temperature event in the Tokyo metropolitan area using numerical simulations: the
612 potential role of a 'hybrid' foehn wind. *Quarterly Journal of the Royal Meteorological*
613 *Society*, 141, 1857-1869. https://doi.org/10.1002/qj.2490.
614 Würsch, M. and Sprenger, M. (2015) Swiss and Austrian Foehn revisited: A Lagrangian-based
615 analysis. *Meteorologische Zeitschrift*, 24(3), 225-242.
616 https://doi.org/10.1127/metz/2015/0647.
617 Yoshino, M. (1975) *Climate in a Small Area – An Introduction to Local Meteorology*. Tokyo:
618 University of Tokyo Press. 549pp.
619 Zängl, G. (2003) Deep and shallow south foehn in the region of Innsbruck: Typical features and
620 semi-idealized numerical simulations. *Meteorology and Atmospheric Physics*, 83, 237-262.
621 https://doi.org/10.1007/s00703-002-0565-7.
622 Zängl, G. (2004) Numerical simulations of the foehn in the Rhine valley on October 24, 1999
623 (MAP IOP 10). *Monthly Weather Review*, 132, 368-389.
624 https://doi.org/10.1175/1520-0493(2004)132<0368: NSOTFI>2.0.CO;2.

Graphical Abstract

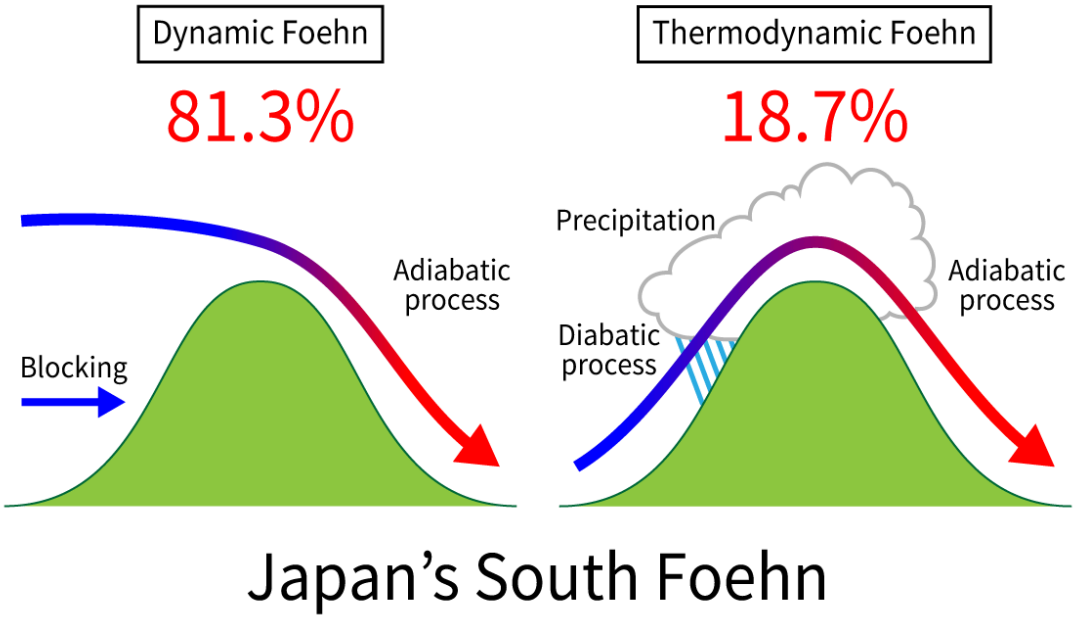

Most (81.3%) of Japan's south foehns blow across the Toyama Plain without precipitation on windward mountain slopes. Approximately 68.2 % of foehns occur when extratropical cyclones pass over the Sea of Japan, while ~19.7% are anticyclonic. Most of the foehns begin blowing at night and end or pause during the day. Air particles primarily descend from the Hida Highlands, between two mountain ranges, as hybrid type of foehns and gap winds.

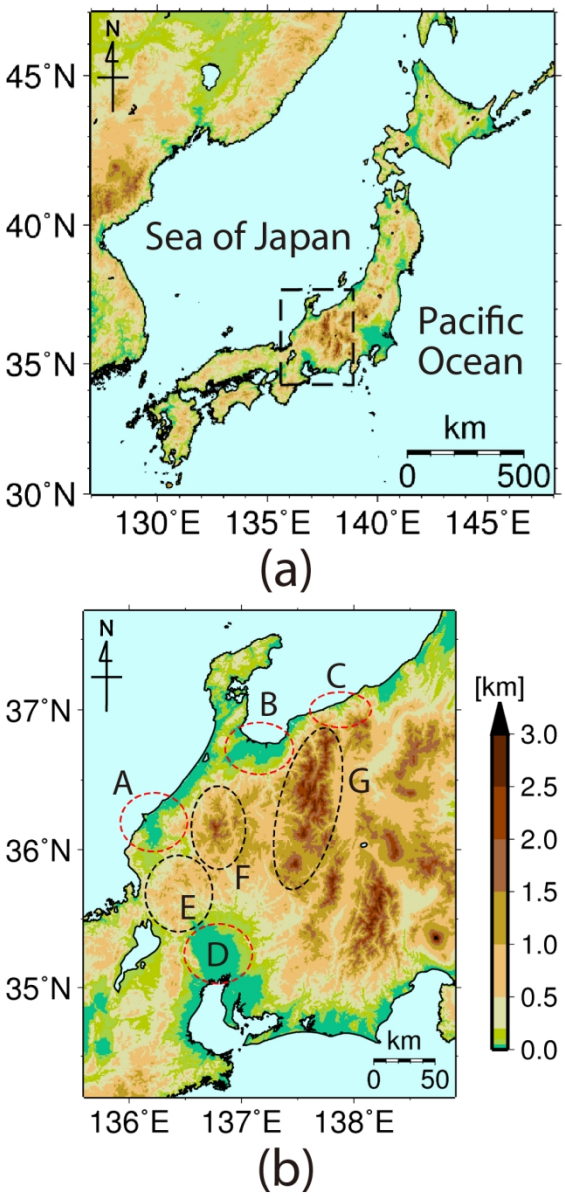

Figure 1. (a) Topography around the main island of Japan (i.e. Honshu). (b) Central region of Honshu. The area near the coast of the Sea of Japan in Fig. 1b corresponds to the Hokuriku region. The red circles, A, B, C, and D, represent the Fukui Plain, Toyama Plain, Itoigawa Area, and the Nobi Plain, respectively. The black circles, E, F, and G represent the Ibuki Mountains, Ryohaku Mountains, and Hida Mountains, respectively. The highlands between F and G are called the 'Hida Highlands'.

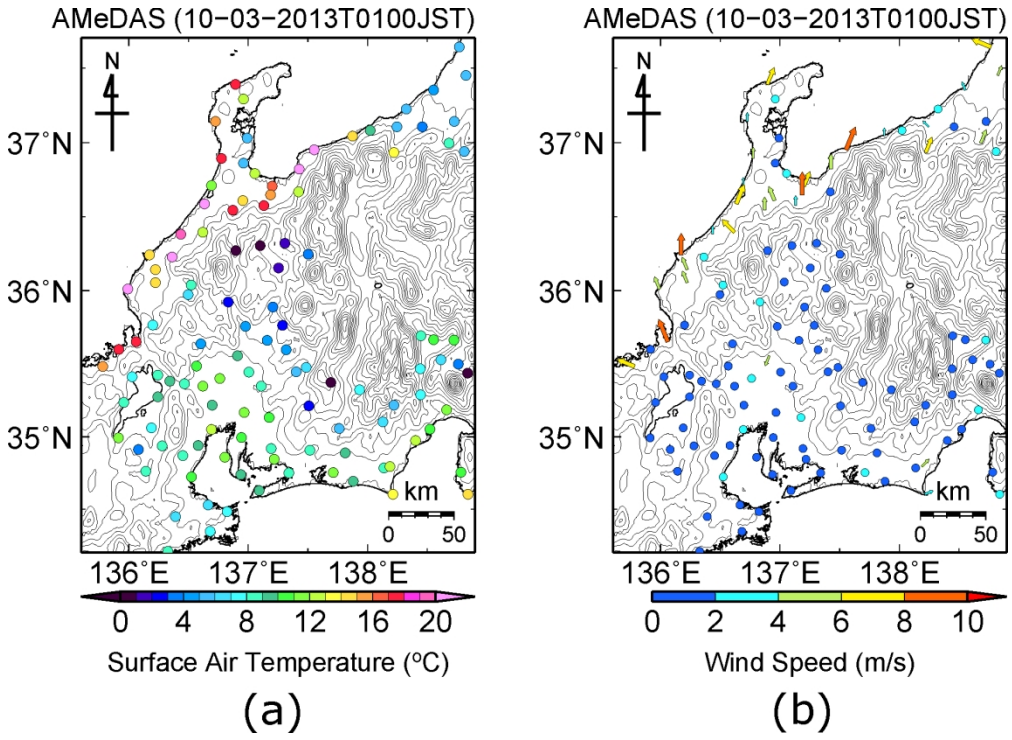

Figure 2. Example distributions of near-surface (a) temperatures and (b) winds obtained from observations during cyclone-induced south foehn events. The solid lines indicate the topography (contour intervals of 200 m).

253x183mm (200 x 200 DPI)

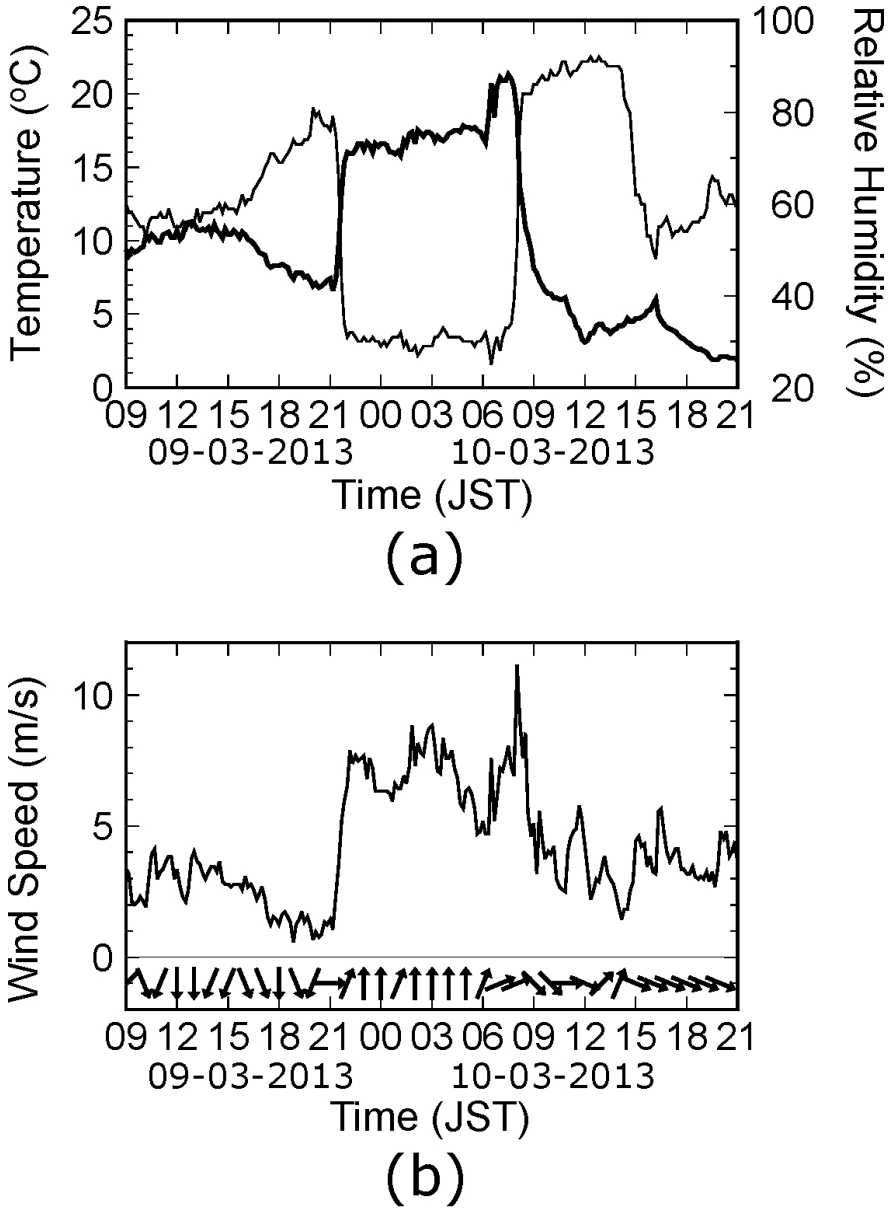

Figure 3. Time series of (a) temperature and relative humidity and (b) wind speed and direction near the surface at the Toyama observatory for cyclone-induced foehns. Thick and thin lines in (a) indicate temperature and relative humidity, respectively. The solid line and vector in (b) indicate wind speed and wind direction, respectively.

143x196mm (200 x 200 DPI)

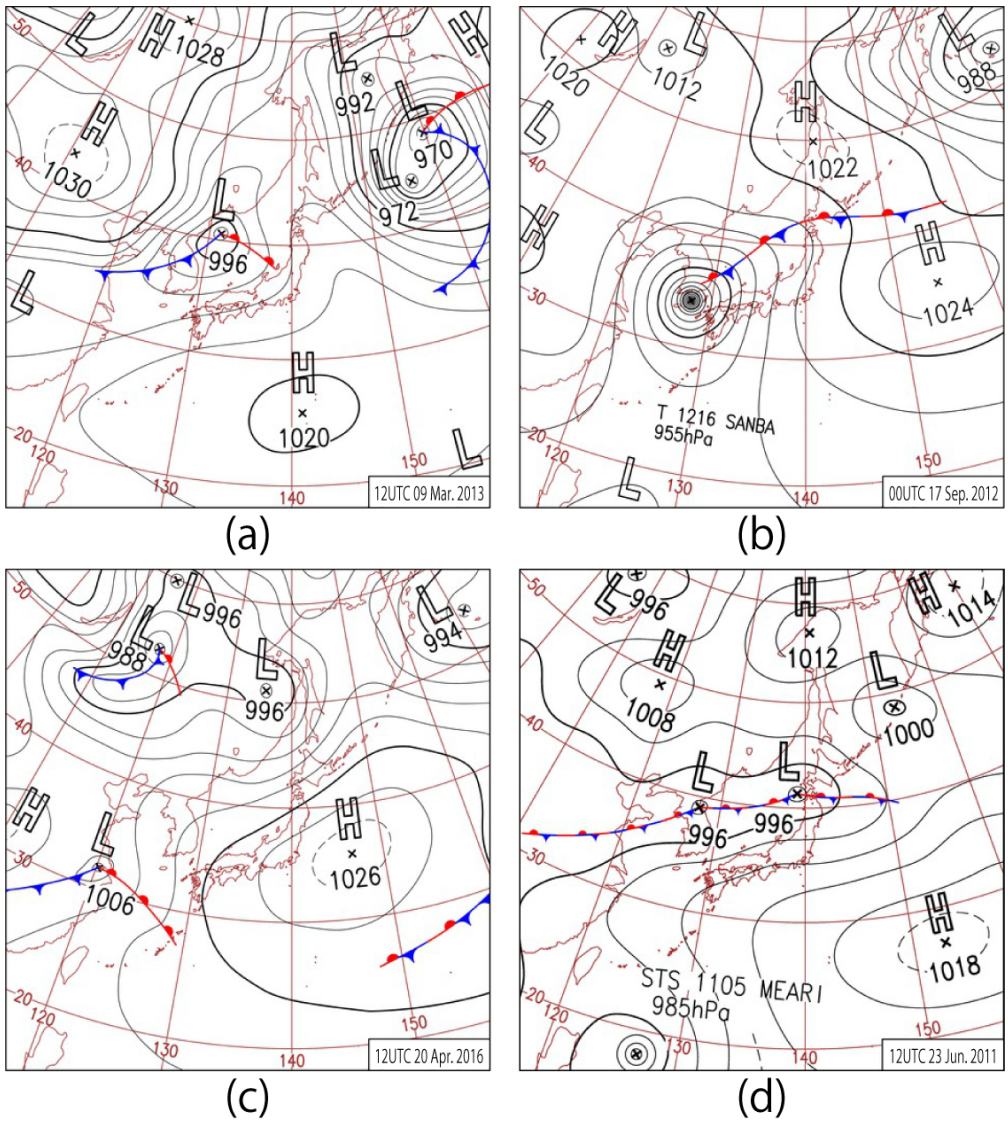

Figure 4. Example synoptic weather charts during foehn events: (a) extratropical cyclone; (b) typhoon; (c) anticyclone; (d) stationary front.

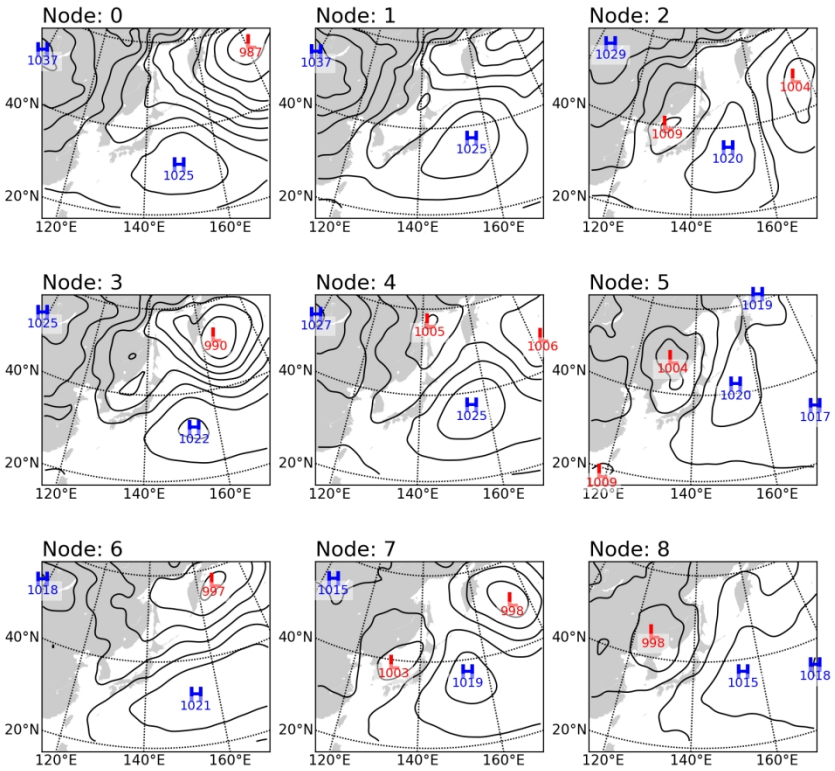

Figure 5. Self-Organised Maps of Nodes 0–8. Maps indicate the sea level pressure patterns proximal to the timing of foehn onset (contour intervals of 4 hPa).

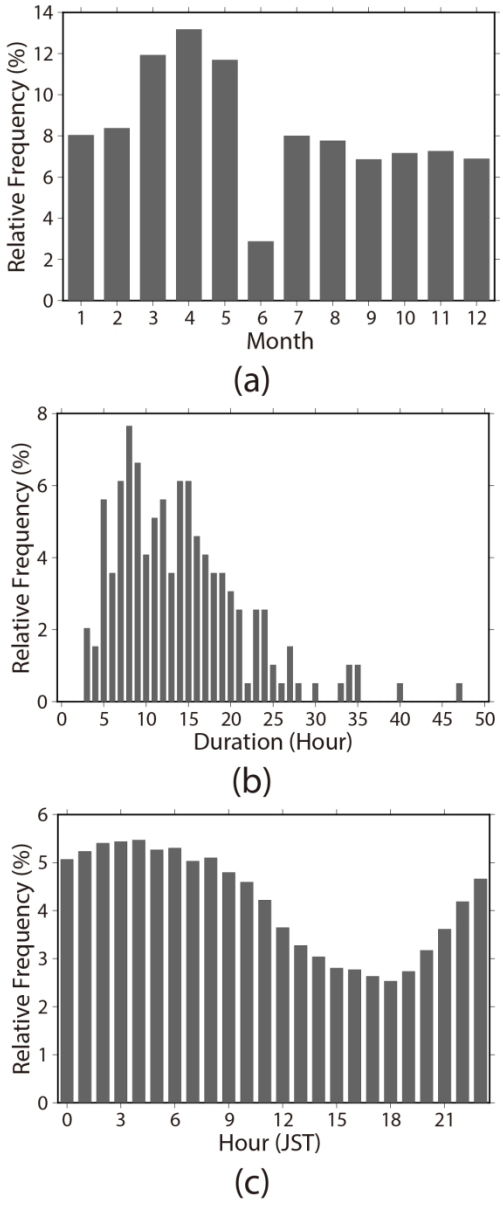

Figure 6. Relative frequencies and durations of Japan's south foehns on the Toyama Plain: (a) monthly; (b) duration; (c) hourly. Grey bars of (a) indicate the data collected at the foehn onsets. Grey bars of (b) and (c) indicate the data collected during foehn events.

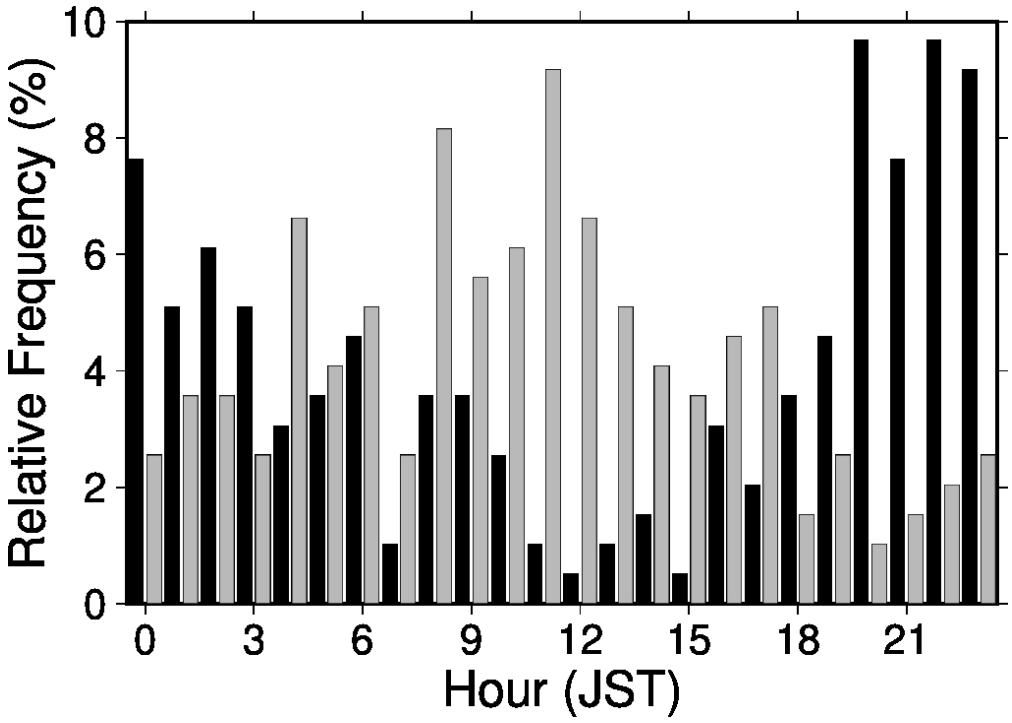

Figure 7. Relative frequencies of the onset (black bars) and end (grey bars) times of Japan's south foehns.

172x122mm (150 x 150 DPI)

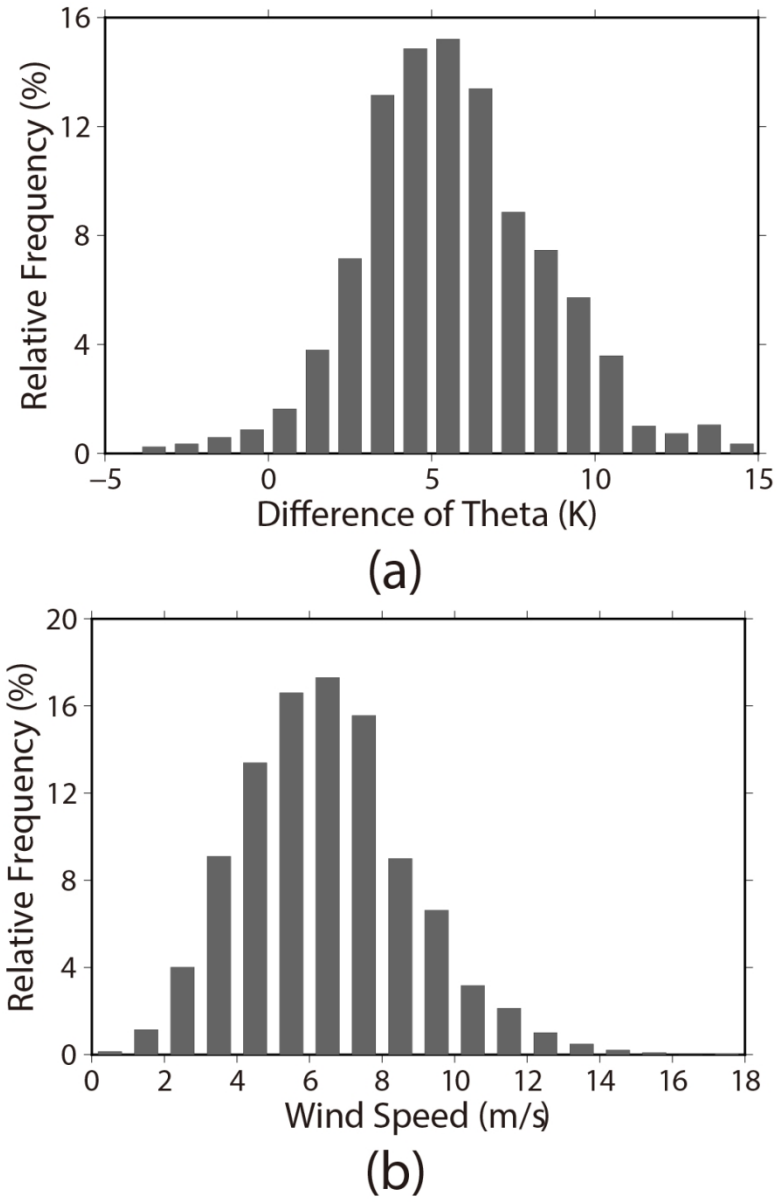

Figure 8. Relative frequencies of the intensity of Japan's south foehns. (a) Potential temperature difference between the stations on the Toyama Plain and Nobi Plain. (b) Wind speed at the Toyama observatory. Grey bars indicate the data collected during foehn events.

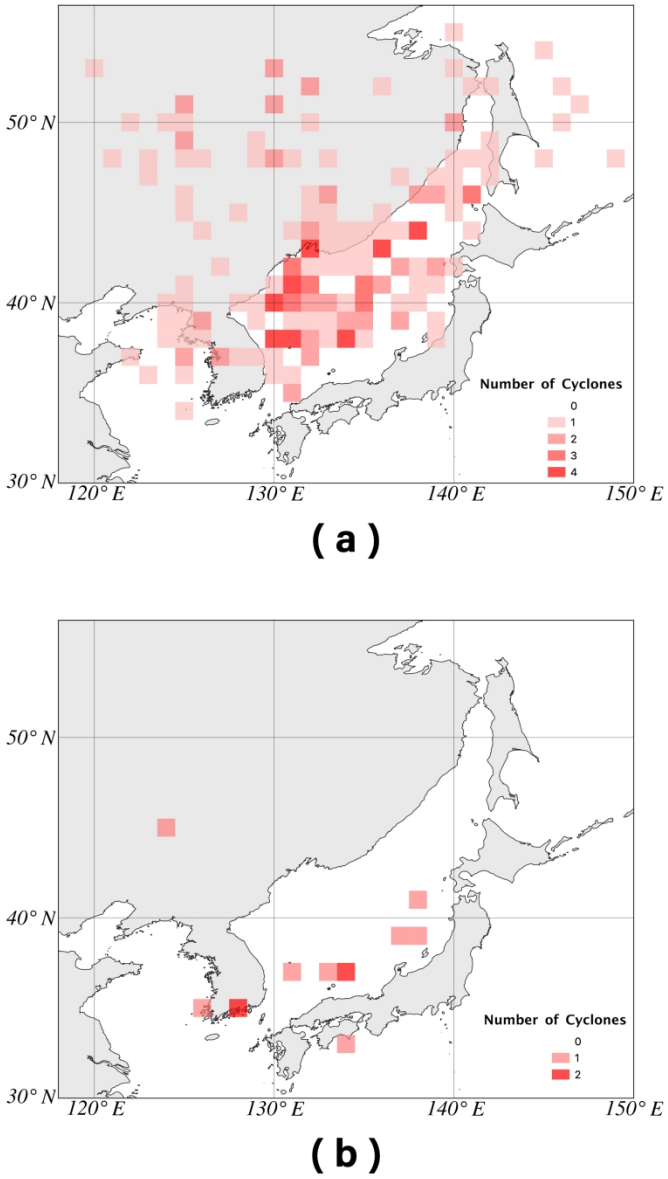

Figure 9. Location of the cyclone centres proximal to foehn onset for cyclone-type foehns (a) without precipitation and (b) with precipitation. Color scales indicate the number of cyclones at each location.

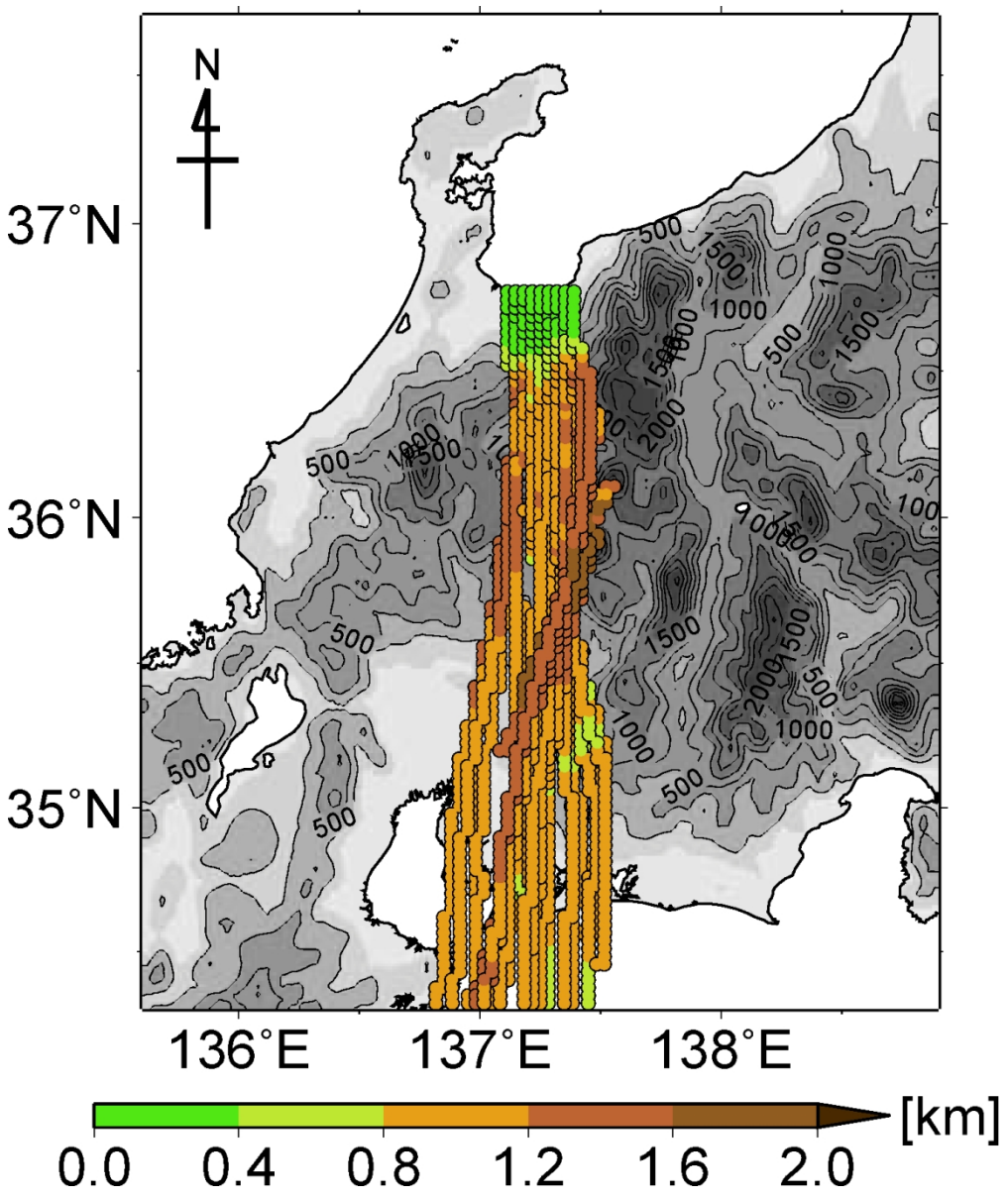

Figure 10. Examples of anticyclonic foehn trajectories without precipitation on the windward side. Colored lines indicate the altitude of the trajectories. Grey scales indicate the topography (contour intervals of 250 m).

164x195mm (230 x 230 DPI)

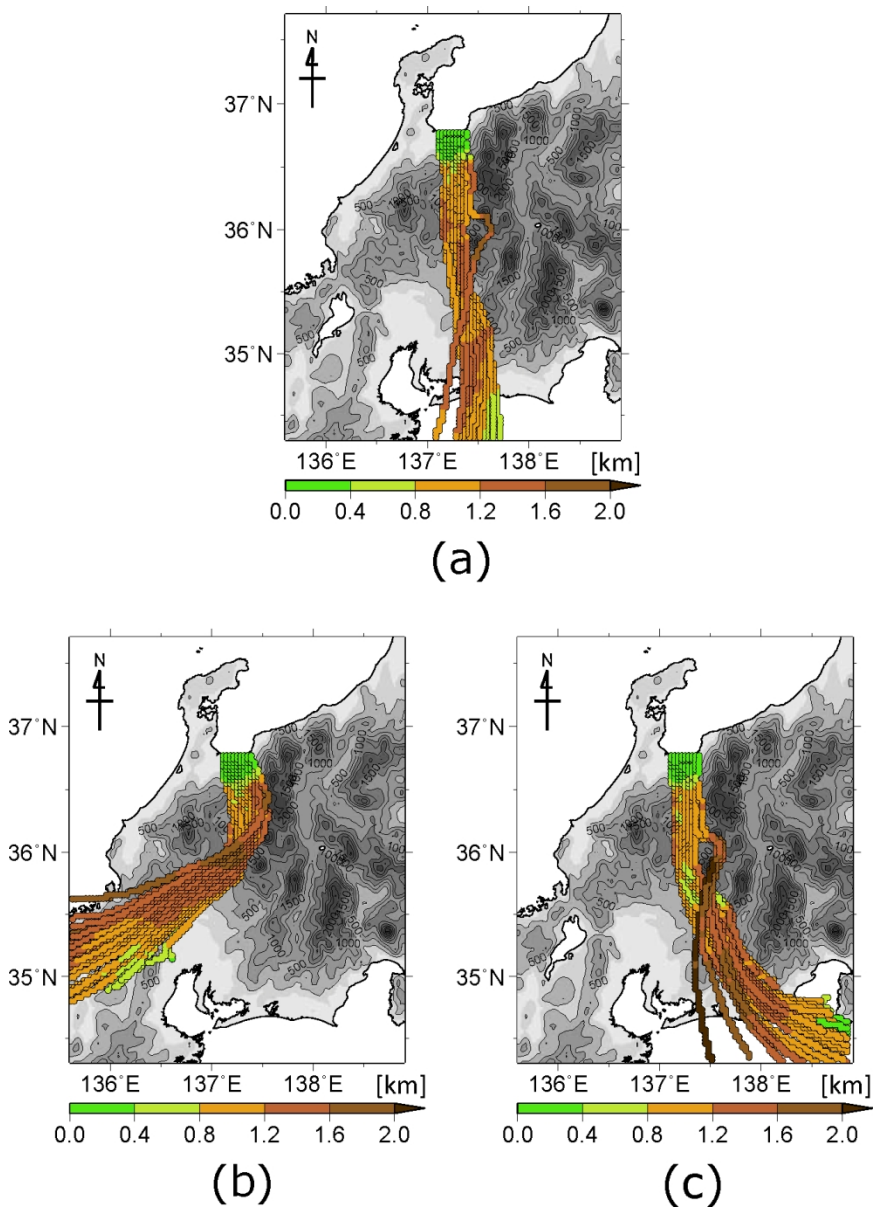

Figure 11. Examples of cyclonic foehn trajectories without precipitation on the windward side: (a) south course; (b) west course; (c) east course. Colored lines indicate the altitude of the trajectories. Grey scales indicate the topography (contour intervals of 250 m).

173x241mm (200 x 200 DPI)

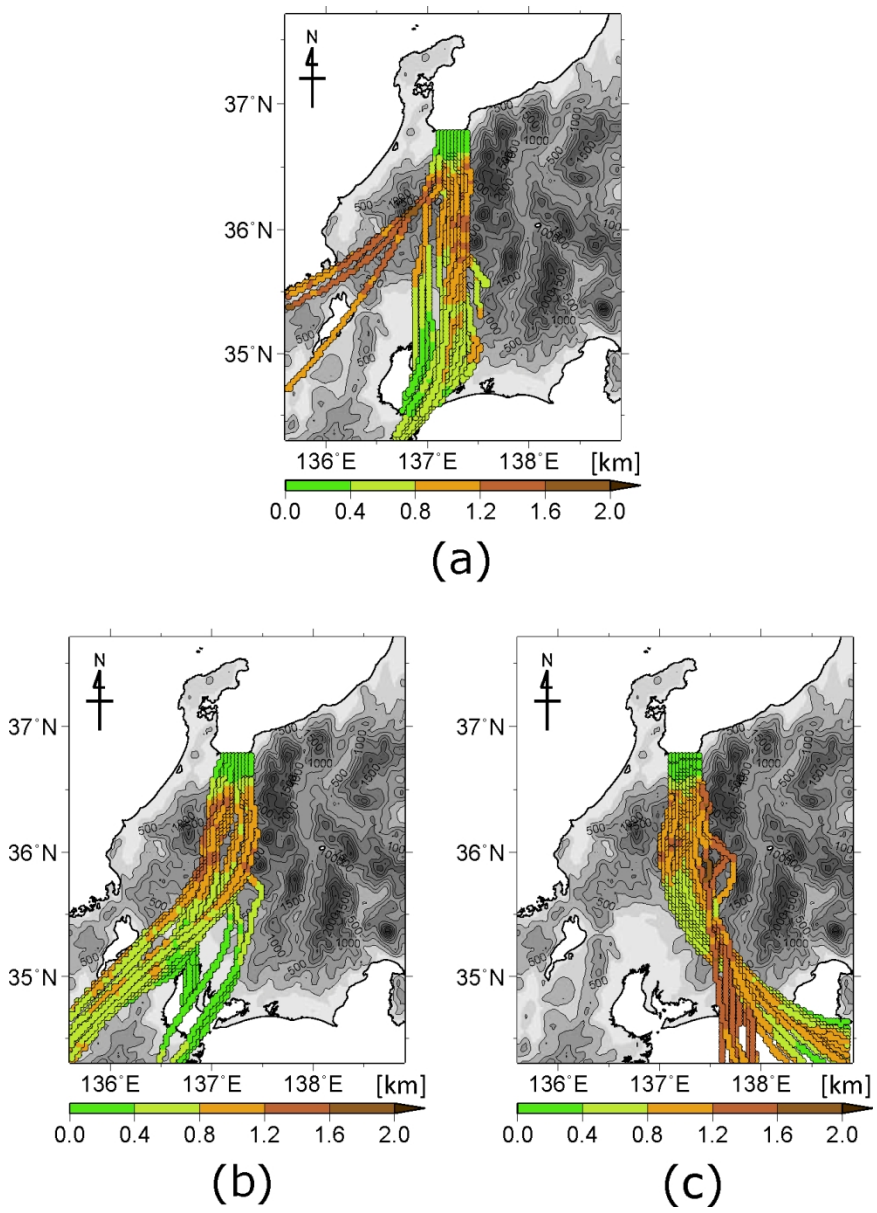

Figure 12. Examples of cyclonic foehn trajectories with precipitation on the windward side: (a) south course; (b) west course; (c) east course. Colored lines indicate the altitude of the trajectories. Grey scales indicate the topography (contour intervals of 250 m).

173x241mm (200 x 200 DPI)

Tables

Table 1. Subjective classification of Japan's south foehn.

	Dynamic w/o precipitation	**Thermodynamic w/ precipitation in the trajectory**	**Total**
Extratropical cyclone	107	28	135 (68.2%)
Anticyclone	39	0	39 (19.7%)
Typhoon	6	4	10 (5.1%)
Other (e.g. Baiu Front, etc.)	9	5	14 (7.1%)
Total	161 (81.3%)	37 (18.7%)	198 (100%)

Table 2. General climatology of Japan's south foehn.

	Primary season (and month)	**Primary onset (% night, 18:00–05:00)**	**Mean duration (hr)**	**Mean, all Δθ (K)**	**Mean, all U (m/s)**
Extratropical cyclone	Spring (April)	71.9%	13.1	5.6	6.5 m/s
Anticyclone	Spring (May)	87.2%	17.8	5.9	6.0 m/s
Tropical cyclone	Summer & autumn (September)	66.7%	13.2	5.7	5.6 m/s
Other (e.g. Baiu Front, etc.)	Summer (July)	78.6%	11.3	4.2	5.2 m/s